

Impact excitation and bottleneck effects in the time-resolved far-infrared photoresponse of high-purity InP

J. M. Chamberlain and A. A. Reeder*

Department of Physics, The University of Nottingham, University Park, Nottingham NG7 2RD, England, United Kingdom

L. M. Claessen,[†] G. L. J. A. Rikken,[†] and P. Wyder[†]

Hochfeldmagnetlabor, Max-Planck-Institut für Festkörperforschung, Boîte Postale No. 166X, F-38042 Grenoble Cédex, France

(Received 3 July 1986)

The time-resolved photoresponse of high-purity ($\mu_{77\text{K}} \approx 10 \text{ m}^2 \text{ V}^{-1} \text{ s}^{-1}$) *n*-type indium phosphide has been investigated at $\lambda = 118.8 \text{ }\mu\text{m}$ with use of a pulsed far-infrared laser. An effective conduction-band lifetime of 60 ns is found which increases slightly in a magnetic field. For sample dc bias voltages exceeding a few volts per centimeter, long tails develop in the photoresponse which last more than 10 μs . The behavior of these tails is examined for various incident laser powers, magnetic fields, and sample bias voltages. It is shown that a four-level model involving impact excitation from impurity states is necessary to describe the photoconductive response. A critical requirement of the model is that the lifetimes of participating "bottleneck" states are 2 and 10 μs . On the basis of known transition probabilities, these bottlenecks are therefore tentatively assigned to the $2p_-$ and $2s$ states.

I. INTRODUCTION

Time-resolved studies of far-infrared photoconduction are a comparatively direct means of examining the dynamical properties of the nonequilibrium distribution following disturbance by pulsed laser excitation. The equilibrium far-infrared (FIR) photoconductivity of InP has been studied for over a decade¹ and has been used as a sensitive assay technique for shallow donor contaminants^{2,3} and to investigate solid-state analogues of the H^- system.^{3,4} Despite this significant interest in equilibrium effects, very little attention has been paid to dynamical measurements in this system.

High-power cw FIR lasers have been used to saturate the $1s$ - $2p_{\pm}$ transitions and the cyclotron resonance⁵⁻⁷ in GaAs; impurity-state and Landau-level lifetimes have been inferred from these measurements assuming appropriate two- or three-level models. It is a conclusion of such measurements for GaAs that very long effective lifetimes of up to 500 ns can be found for the $2p_-$ state which acts effectively as a "bottleneck" in the recombination process.

Although no saturation-absorption measurements have been described for InP, Ohyama *et al.*⁸ have reported extremely long ($\sim 5 \text{ }\mu\text{s}$) lifetimes for conduction-band electrons in InP using FIR pulses synchronized with an external electric field and/or flashlamp. The possible existence of such long lifetimes in InP, and the likely consequences for the kinetics of the shallow donor photoconduction process, motivated an examination⁹ of pulsed FIR photoconductivity in very-high-purity InP. The present article presents additional experimental information and provides a mechanism to explain the long "tails" which could be seen in the photoresponse. A model involving multiple

reexcitations into the conduction band is developed which implies the presence of two bottleneck states. Numerical simulations of the photoresponse based on this model are presented and compared with the experimental data.

Section II describes the electrical properties of the samples and the experimental arrangement. The results are presented in Sec. III and the discussion of these data falls into two parts. Section IV A analyses the behavior of the short-term ($< 1 \text{ }\mu\text{s}$) photosignal in comparison with the behavior of GaAs, and provides an explanation of characteristic "overshoot" effects of the photoresponse with respect to the laser stimulus. Section IV B fully describes the model which is used to explain the long-term ($> 1 \text{ }\mu\text{s}$) photoconductivity. It is shown that the results obtained by this model depend critically on the values of the transition rates involved, which are consistent with reported values in the literature.

II. EXPERIMENTAL

Samples of very-high-purity indium phosphide¹⁰ were provided with four Ohmic contacts: The electrical characteristics of these three samples are given in Table I.

The specimens were mounted in a 4.2-K immersion cryostat in a magnetic field with light pipe access. An electrically pulsed *Q*-switched (*EQ*-switched) CO_2 laser¹¹ was used to pump a FIR waveguide laser with CH_3OH as the active medium. The system provided $118.8\text{-}\mu\text{m}$ -wavelength pulses of variable length (75–500 ns) with a repetition rate of 300 Hz. The maximum FIR power at the sample was 500 mW, which corresponds to an intensity $\sim 5 \text{ W cm}^{-2}$. In most of the present experiments the specimen bias arrangements were configured in a constant current mode, although the constant voltage mode was

TABLE I. Characteristics for different samples.

Sample	$(N_D - N_A)/\text{cm}^{-3}$ (at 300 K)	$(N_D - N_A) \text{ cm}^{-3}$ (at 77 K)	$\mu/\text{cm}^2 \text{V}^{-1} \text{s}^{-1}$ (at 300 K)	$\mu/\text{cm}^2 \text{V}^{-1} \text{s}^{-1}$ (at 77 K)	Thickness (μm)
No. 1 (NAG 755)	2×10^{14}	2.3×10^{14}	4840	114 000	8
No. 2 (NAG 761)	1.6×10^{14}	1.6×10^{14}	4700	129 000	13
No. 3 (NAG 765)	1.1×10^{14}	1.1×10^{14}	4800	123 000	10

also used on occasion. Figure 1 shows the general experimental system: The ac photoresponse of the sample is examined with a boxcar after preliminary amplification by a wide-band preamp. The boxcar is triggered by the laser EQ switch, and a lockin is finally used to provide synchronous amplification. The response characteristics of the measurement system were thoroughly investigated with dummy samples to ensure there were no artefacts in the experimental response. Particular attention was paid to the minimization of stray electromagnetic pulses from the laser, and to the possibility of "geometrical" or electronic artefacts in the time-resolved response.

III. RESULTS

The photoconductive response as a function of time for a typical InP sample (No. 3) is shown in Fig. 2. The sample dc bias is in this case well below the threshold value for impact ionization or excitation effects. For the narrowest laser stimuli the decay is adequately represented by a single exponential with characteristic time τ . Examination of the photoresponse as a function of incident laser power indicates that τ is independent of laser intensity. The application of a magnetic field of 3.75 T (i.e., the resonant field for the $1s-2p_+$ transition when $\lambda=118.8 \mu\text{m}$) produces a small, albeit significant, increase in τ for the same sample under identical bias and illumination conditions. Average values of τ for $B=0$ and 3.75 T are 125 and 150 ns. Effective conduction-band lifetimes are obtained from these values in Sec. IV A. The magnetic field has no effect, within the limits (~ 20 ns) of experimental observation, on the rise profile of the pulse.

The photoresponse of a sample of n -GaAs type ($N_D - N_A = 2 \times 10^{15} \text{ cm}^{-3}$) was used to monitor the FIR laser output. Maan¹² has shown that this sample is capable of following the laser pulse. The development of the InP photosignal as a function of time is shown in Fig. 3

for increasing pulse widths and constant peak power. The breakdown in the simple exponential decay shape is evident for the widest photoresponses observed. The figure also indicates, for a particular InP response curve, the profile of the FIR laser stimulus. A characteristic overshoot between the maxima of stimulus and response is noted. Care was taken to ensure that this was not an artefact of the experimental geometry or signal-retrieval systems. The overshoot was found to increase approximately linearly with the integrated energy of the input pulse as shown in Fig. 4.

The comparatively simple photoresponse signal was observed to develop additional structure when the sample bias was raised above a characteristic threshold value V_T corresponding to a sample electric field of the order 1 V cm^{-1} . Figures 5 and 6 show the development of these "tails" for $B=0$ and 3.75 T. The noise pattern in the tail is strongly suggestive of a random multiplication process. In some cases, dependent on compensation ratio and bias, the signal height of the tail was found to exceed that of the initial photoresponse. The existence of a prominent tail was noted at magnetic fields between 0 and 6 T: the shape of the tail is not resonant with $1s-2p_+$ signal. V_T was found to increase approximately linearly with magnetic field, and this strongly suggests the participation of impurity states in the tail mechanism. Similar observations of the tail were also made at 2 K. The photoresponse tails were seen in all the samples used with varying patterns and types of electrical contact.

The dependence of the photoresponse on magnetic field at different times after excitation was investigated. Figure 7 indicates the difference in spectral information carried in the initial pulse and the tail: it is apparent that only a small amount of information is carried in the tail, whereas the short-term response displays more strongly the $1s-2p_+$ transition.

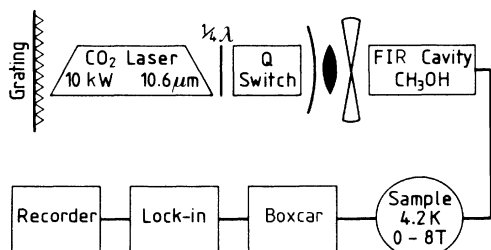
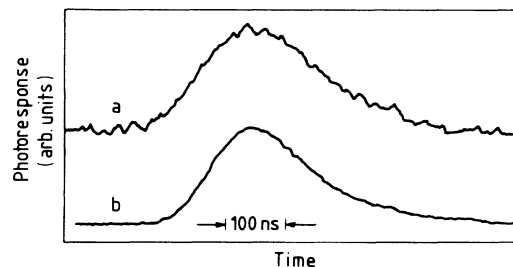


FIG. 1. General experimental arrangement.

FIG. 2. Photoconductive response of sample No. 3 below V_T at 4.2 K. (a) 3.75 T; (b) 0 T.

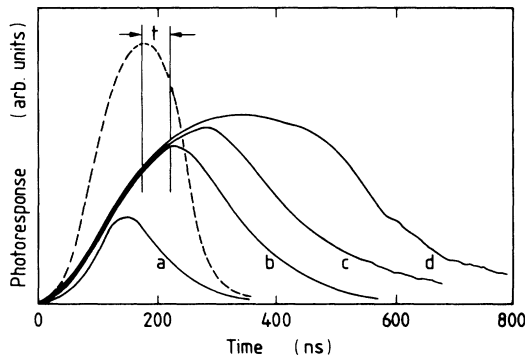


FIG. 3. Development of short-term photoresponse of sample No. 3 at 4.2 K for increasing input pulse width. The stimulus pulse for one particular response (b) is shown as a dotted line, and the overshoot t is indicated.

The effects on both the initial and tail photoresponses when the incident laser power was varied were examined for the $B=0$ and 3.75 T cases. Figure 8 shows this variation for samples No. 3 and 1 at 3.75 T. It is evident that the initial photoresponse is beginning to saturate for laser powers $>5\%$ of maximum. The tail, however, displays markedly different properties. In a magnetic field the tail photoresponse remains constant over some two to three orders of magnitude change in incident laser intensity, whereas at zero field it decreases superlinearly.

The tail is believed to originate (next section) from a multiplication and "recycling" process which is random in nature, the efficiency of which would seem to be dependent on sample compensation ratios. It was, in some samples, difficult to establish the tail photoresponse in zero applied magnetic field.

IV. DISCUSSION

A. Mechanism for the initial photoresponse ($t < 1 \mu\text{s}$)

The conventional processes of optical excitation and photoconduction are considered to be responsible for the

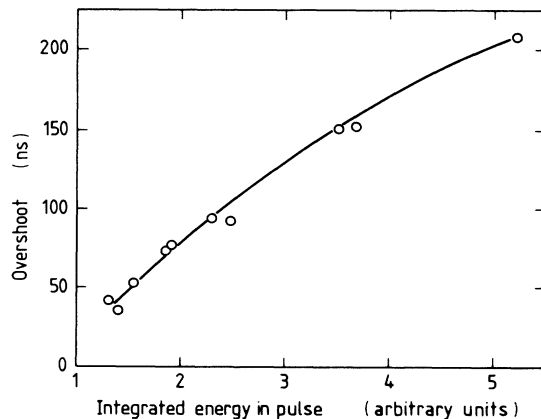


FIG. 4. Graph of overshoot versus integrated input pulse energy for sample No. 3 at 4.2 K.

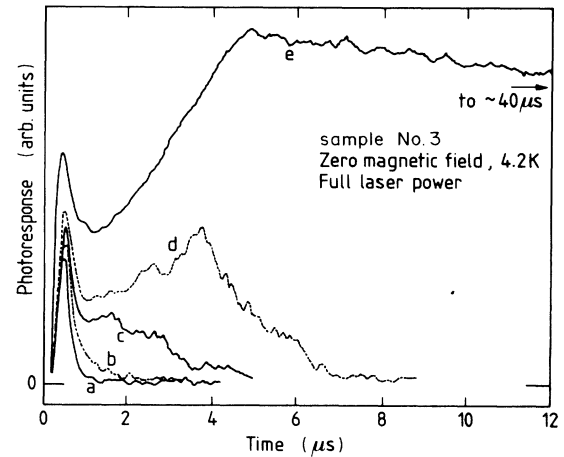


FIG. 5. Characteristic tail patterns at 4.2 K, for sample No. 3 at $B=0$ T. The conditions of sample bias are (a) 1.2 V cm^{-1} , (b) 1.4 V cm^{-1} , (c) 1.6 V cm^{-1} , (d) 1.8 V cm^{-1} , and (e) 4 V cm^{-1} .

initial photoresponse observed in Fig. 2. The photoexcitation process occurs in a characteristic time τ_{1c} , given by $\tau_{1c} = (\sigma_{1s} F)^{-1}$, where F is the photon flux and σ_{1s} the photoionization cross section. With values of F and σ_{1s} ($\approx 10^{-12} \text{ cm}^2$) (Ref. 6) appropriate to these conditions, τ_{1c} is much less than 1 ns. Using simple order-of-magnitude arguments and the known sample impurity concentration, it may be shown that a significant fraction ($>50\%$) of the donors are ionized by the laser pulse. This is consistent with the observation (Fig. 8) that the initial peak in the photoresponse begins to be saturated when $(I/I_0) > 5\%$. Furthermore, the sample resistance (as calculated from the photosignal during saturation) closely matches the minimum obtainable dc resistance due to thermal ionization of donors, hence supporting the argument that a very large fraction of the donors is ionized.

At zero magnetic field, injection into the conduction band is at approximately 2.5 meV. An effective carrier temperature T_e is established within $\sim 10^{-11}$ s by carrier-carrier scattering.^{6,7} The warm electron gas gains further energy from each optically excited electron and from dc carrier heating, losing energy by acoustic phonon

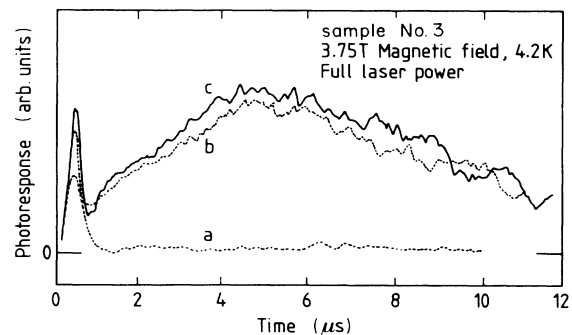


FIG. 6. Characteristic tail patterns at 4.2 K for sample No. 3 at $B=3.75$ T. The conditions of sample bias are (a) 4 V cm^{-1} , (b) 6.8 V cm^{-1} , and (c) 10 V cm^{-1} .

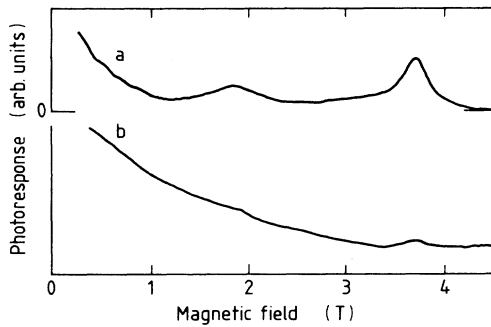


FIG. 7. Photoconductive response versus magnetic field for sample No. 2 at 4.2 K. (a) Short-term response; (b) tail response.

emission. Under present conditions this total heating rate is estimated at $3 \mu\text{W}$. The analysis of McManus *et al.*¹³ provides an approximate value of $T_e \approx 5 \text{ K}$, assuming 10^{-9} s as the time for acoustic phonon emission^{13,14} under the present conditions. Electrons in the gas eventually deexcite through excited impurity states: The possibility of thermal reexcitation is not considered to be significant in this case.

To obtain an absolute value from the present measurements for the conduction effective lifetime τ' in InP at zero field under low bias conditions, it is necessary to deconvolve the laser decay profile from the experimental data of Fig. 2. A reasonable estimate may be made by noting the difference in decay times (50 ns) for the InP sample and GaAs detector, and assuming an effective lifetime of 10 ns in GaAs.⁶ The effective lifetime is therefore 60 ns, a value supported by more recent experiments which directly measure this lifetime.¹⁵ Consequently τ' at the resonant magnetic field will be 85 ns. The subsequent decay to the ground state occurs predominantly by phonon emission through excited states:¹⁶ This process will be discussed more fully in the next section.

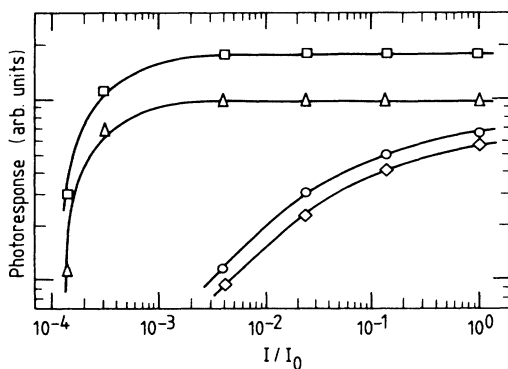


FIG. 8. Effects of varying laser power (I/I_0) on tail and short-term response for two samples at 4.2 K and $B=3.75 \text{ T}$. \square : sample No. 1, tail. Δ : sample No. 3, tail. \diamond : sample No. 3, short term. \circ : sample No. 1, short term.

The characteristic “overshoot” in the photoresponse with respect to the stimulus (Fig. 4) has been investigated as a function of the integrated energy in the laser pulse. The effect is observed in a number of samples: A suggested explanation is that the overshoot represents an effective time (t) during which the electron mobility rises as the number of acoustic phonons (emitted by the rapidly cooling electron population) diminishes. The acoustic phonon population is created within a few nanoseconds of optical excitation and leaves the epilayer during the time t . Using a simple kinetic theory argument, the time for ballistic ejection from an epitaxial layer of thickness l is

$$t_0 = \frac{l}{v_s}, \quad (1)$$

where v_s is the velocity of sound. This time is increased by a factor (l/λ) , where λ is the phonon mean free path. λ will diminish with increasing phonon population, i.e., at higher laser powers. Thus

$$t = l^2 / v_s \lambda. \quad (2)$$

Using values of $l = 10 \mu\text{m}$, $v_s = 10^3 \text{ m s}^{-1}$, and $\lambda \approx \frac{1}{2} \mu\text{m}$ (deduced from the greatest number density of optically excited carriers), an order-of-magnitude value of 60 ns is obtained, consistent with the observed overshoot.

A slight increase in the decay time of the short-term response is noted in the resonant field of 3.75 T. This is probably attributable to decreased transition probability as the conduction-band wave functions shrink in the magnetic field.

Since the $N=0$ Landau level lies at a lower energy than the $2p_+$ state, at 3.75 T, the transfer of electrons into the conduction band takes place by either tunneling or phonon emission. Saturation-absorption measurements for GaAs (Ref. 6) at the resonant field for the $1s-2p_+$ transition imply that this process occurs in $\sim 20 \text{ ns}$ in GaAs, so that a slight increase in signal rise time (with respect to measurements at $B=0$) might also be expected in the InP samples. However, although this is not within the resolution of the present experimental arrangement, recent preliminary measurements¹⁵ with a 3-ns resolution system show no such increase in rise time at the resonant field.

B. Mechanism for the long-term photoresponse ($t > 1 \mu\text{s}$)

The fundamental mechanism thought to be responsible for the “tails” in the photoresponse at $V > V_T$ is impact excitation of neutral donors at a relatively low ($1-2 \text{ V cm}^{-1}$) bias field. This process is distinct from “normal” impact ionization which will occur at somewhat higher bias fields. It was first invoked to explain changes in the magnetoresistance of epitaxial n -type GaAs.¹⁷ The changes in excited-state populations produced by this mechanism in GaAs have very recently been investigated using far-infrared spectroscopy.¹⁸ The process envisages multiple reexcitations from excited states: We extend this idea to consider an avalanche process leading to the observed increases in sample photoresponse which can continue for very long periods (up to $\sim 40 \mu\text{s}$ in some cases).

In the only other report known to the present authors of “tails” in the submillimeter photoresponse of a semi-

conductor, Brown *et al.*¹⁹ ascribe the effect to electrons trapped in a hybrid impurity band. Impurity band conduction is known to decrease substantially in magnetic fields,²⁰ typically by a factor of 15 in fields of 2 T, so that some reduction in tail signal might be expected. Since the tail is seen to be prominent at magnetic fields of up to 6 T, this is unlikely to be the operative mechanism in our case. Furthermore, impurity banding in these samples is unlikely due to their low doping concentration (see Table I).

The approximately linear increase in V_T as the magnetic field is raised is consistent with an initiating process such as impact excitation from a population of electrons in a $2s$ state. The mechanism will then proceed in an essentially random fashion, with carrier multiplication into the conduction band from impact-excited electrons in higher-lying excited impurity states. The photosignal rapidly (4–5 μ s) attains a maximum value representing a dynamic equilibrium between excitation and trapping processes: Some variation in the maximum value of this photosignal is therefore to be expected as the efficiency of the conduction-band multiplication process will be dependent on sample compensation ratios.

A simple rate-equation formalism was used⁹ to account for the temporal characteristics of the tail. The conduction-band population was obtained from the numerical solution of three coupled rate equations describing electron populations in the ground state, the conduction band, and a suitable bottleneck impurity state. The fitting parameters of these equations were consistent with reported lifetimes^{6,16} of appropriate bottleneck states for zero field and 3.75-T measurements. The evidence of Fig. 7, that there is very little spectral information present in the tail, is considered to be generally supportive of the “carousel” mechanism giving rise to the tail, as such spectral information will be lost in the repeated excitation and trapping processes.

The carousel mechanism invokes a single crude “return” parameter to account for carrier impact excitation into the conduction band. This single parameter requires refinement to adequately represent the complex excitation process alluded to above. For instance, one consequence of this oversimplification is that the simple rate-equation simulations⁹ cannot satisfactorily account for the incident laser power versus photosignal characteristics (Fig. 8) or for the marked variation of these characteristics in a magnetic field.

A further attempt was therefore made to model the kinetic processes prevalent at the outset of the impurity breakdown in order to explain the general shapes of the observed tails and, in particular, the remarkable result (see Fig. 8) that the tail signal in a magnetic field is sustained over several orders of magnitude reduction in the stimulating laser power level.

It is proved that the photoresponse in a magnetic field can be most simply explained by invoking a four-level model as shown in Fig. 9. The rate equations pertinent to this model are

$$\frac{dn}{dt} = -\alpha n(n + N_A) + rnN_3 + SN_1, \quad (3)$$

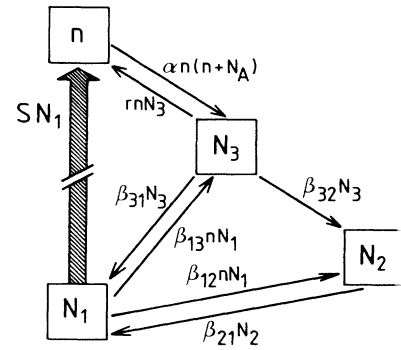


FIG. 9. Model of recombination and impact excitation processes. Only those transition rates relevant to the present model are indicated. n is the conduction-band population, N_1 the impurity ground-state population, and N_2 and N_3 populations of excited states (see text). N_A is the acceptor concentration.

$$\frac{dN_1}{dt} = -\beta_{12}nN_1 + \beta_{21}N_2 + \beta_{31}N_3 - \beta_{13}nN_1 - SN_1, \quad (4)$$

$$\frac{dN_2}{dt} = \beta_{32}N_3 - \beta_{12}nN_1 - \beta_{21}N_2, \quad (5)$$

$$\frac{dN_3}{dt} = \alpha n(n + N_A) - rnN_3 - \beta_{32}N_3 + \beta_{13}nN_1 - \beta_{31}N_3. \quad (6)$$

The source term (S) representing the initial input of electrons into the conduction band by the FIR pulse was taken as a Lorentzian of appropriate half width. Equations (3)–(6) above were solved numerically and computer-generated simulations of the photoresponse of InP were obtained for a variety of parameter choices. Results of these simulations are shown in Fig. 10 for zero magnetic field and at 3.75 T. For ease of comparison, appropriate experimental tails are also plotted on this figure. The inset of Fig. 10 presents a graph of the maximum simulated photosignal at 3.75 T as a function of the incident laser power for both the short-term and tail components. It is evident from the figure that Eqs. (3)–(6) can satisfactorily account for the presence of a tail at low laser powers even when the short-term photoresponse has virtually disappeared.

A direct mathematical analysis demonstrates the need to assume a fourth “level” to account for the eventual decay of the tail. It may be shown that such a long-term decay will not occur with three “levels.” It is assumed that the dominant process for the production of long-lived tail is the inelastic scattering of electrons from the impurity ground state (population N_1) into an excited state or group of states represented by the population N_3 . A subsequent ionization into the conduction band may then occur which is represented by the rate parameter r , as in the three-level model.⁹ The present model, however, requires the existence of a second state (or group of states) at an intermediate energy and for which the electron population is N_2 . Slow recombination processes to the ground state are then invoked to explain the eventual de-

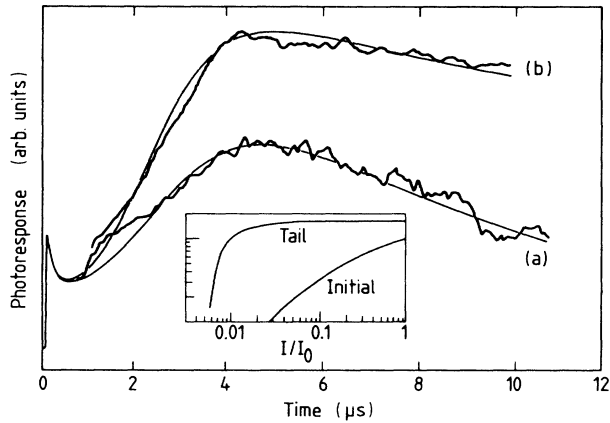


FIG. 10. Simulations of photon conductivity. Appropriate experimental data are reproduced for comparison. Curve (a) is simulation for the resonant magnetic field: $\alpha=6\times 10^{-8}$ cm^3s^{-1} , $r=6\times 10^{-8}$ cm^3s^{-1} , $\beta_{32}=2\times 10^5$ s^{-1} , $\beta_{21}=10^5$ s^{-1} , $\beta_{12}=3\times 10^{-9}$ cm^3s^{-1} , $\beta_{13}=7.2\times 10^{-9}$ cm^3s^{-1} , $\beta_{31}=5\times 10^5$ s^{-1} . The initial $N_1=2\times 10^{14}$ cm^{-3} and $N_a=3\times 10^{13}$ cm^{-3} . Curve (b) is a simulation for zero field for which $\beta_{32}=0$ s^{-1} . The inset shows simulated saturated data for tail and initial response at 3.75 T.

cay of the tail over several tens of microseconds. The physical justification for the choice of parameters used in the simulations and the possible nature of the states represented by the populations N_2 and N_3 will now be considered.

The analysis of Ascarelli and Rodriguez¹⁶ concludes that in zero magnetic field the $2s$ state acts as an effective bottleneck in the phonon-assisted recombination process. However, in a magnetic field it is likely that the lower-energy $2p_-$ state can also act as a bottleneck and this is supported by the lifetime measurements of Allan *et al.*⁶ for GaAs. It is therefore reasonable to suggest an assignment of the population N_2 to the $2p_-$ state and the population N_3 predominantly to the $2s$ state: The consequences of the degeneracy of these states at $B=0$ will be examined later. Calculations of the $2p_-1s$ and $2s1s$ lifetimes for InP using the analysis of Ascarelli and Rodriguez,¹⁶ and an appropriate deformation potential,²¹ yield values of 10 and 2 μs , respectively. The decay parameters β_{21} and β_{31} were chosen using these lifetimes for the simulations of Fig. 10. The chosen conduction-band decay parameter α is consistent with the effective lifetime of 60 ns obtained from the short-term response measurements. The critical dependence of the resulting shape of the photoresponse curve on the value of the parameters used in the model will be discussed shortly.

The chosen values of the impact excitation parameters r , β_{13} , and β_{12} are in general agreement with those reported by Scholl.²² It is possible to comment on the relative sizes of some of these parameters by analogy with the reported cross sections for electron impact in atomic hydrogen.²³ Such comparisons indicate that the cross section for $1s2p_-$ excitation is at least a factor of 3 smaller than for either $1s2s$ or $1s2p_0$ excitations, which is consistent

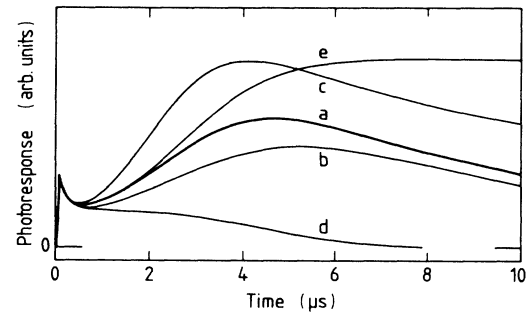


FIG. 11. Simulations of the photoconductive response for a variety of model parameters. Curve *a* has the same parameter choice as curve (a) of Fig. 10. (I.e., transition times 2 and 10 μs for $2s1s$ and $2p_-1s$, respectively). Curve *b* as curve *a*, but all impact excitation parameters reduced by 5%. Curve *c* as curve *a*, but $2s1s$ transition time equals 5 μs . Curve *d*, $2s1s$ transition time 1 μs . Curve *e*, $2s1s$ transition time equals 2 μs and $2p_-1s$ transition time equals 2 μs .

with the relative chosen values for β_{12} and β_{13} and with the tentative assignments of the N_2 and N_3 populations previously discussed. Finally, it is noted that the faithful simulation of the experimentally observed tail requires a minimal impact ionization of the N_2 states(s): This is implied by simple consideration of angular momentum conservation and wave-function symmetry.²⁴

Figure 10 displays a photocurrent simulation in which the parameter β_{32} is set at zero. The striking similarity between this computer-generated plot and the zero magnetic field data implies a zero transfer rate between the N_3 and N_2 populations in zero magnetic field, which is to be expected from the degeneracy of the $2s$ and $2p_-$ states and the population assignments previously discussed.

The critical dependence of the simulations on the choice of the relevant parameters will now be considered. The model proposed in Fig. 9 shows only those transitions which are numerically found to have a substantial influence on the photoconductive response. Figure 11 shows the effects of varying several parameters for a photoresponse simulation at 3.75 T. Curve *a* shows the simulation which most closely resembles the experimental data (see Figs. 10 and 6). Curve *b* represents a slight decrease in the impact excitation parameters corresponding to lower sample bias conditions. The curves *c*, *d*, and *e* demonstrate the effects of varying the recombination rates. The criticality of the choice of parameters is evident from the figure.

The simulations based on Eqs. (3)–(6) provide a reasonable description of the tail behavior with the correct choice of parameters. However, the short-term response (<1 μs) is not so well represented by the present model and there are two major reasons for this. The first is that the simulations do not take into account the overshoot effects discussed in Sec. IV A, which are important on this time scale. The second is that the model assumes instantaneous capture by the state, whereas in reality a cascade through a sequence of short-lived states will occur.

There was some experimental evidence that tail formation in zero field was more difficult to establish and had a greater susceptibility to sample variation and laser power than tail formation at the resonant magnetic field. Although this behavior is not fully understood, it is suspected to be related to the relative magnitudes of the slightly higher bias required in a magnetic field and the random internal electric fields²⁵ associated with the ionized impurities. It was not possible, however, to apply a comparable high bias at zero field, because of the onset of total breakdown produced by direct impact ionization of the ground state. The noisy appearance of the tail, particularly at long ($> 5 \mu\text{s}$) times is perhaps a manifestation of the onset of filamentary conduction processes which have been observed in GaAs (Ref. 26) and Ge (Ref. 27).

V. CONCLUSIONS

The photoconductive response of three high-purity n -type InP samples has been studied at 4.2 K using 75–500-ns pulses of 118.8- μm radiation from a CO_2 pumped FIR laser. At low sample bias voltages the photoresponse is a slightly asymmetric pulse represented by a simple exponential decay of characteristic times 125 and 150 ns at 0 and 3.75 T, respectively, which correspond to effective lifetimes of 60 and 85 ns. The significance of these times relative to other measurements in GaAs is discussed. The development of this photosignal was monitored as a function of the laser stimulus power, and overshoot effects were observed where the sample photoconductance continued to increase for a period (or order 50 ns) while the stimulus power fell. The effect was seen to be approximately proportional to the magnitude of the input power integrated over the laser pulse period. This was interpreted as the characteristic time during which the electron mobility rose while acoustic phonons were ejected into the substrate.

At sample bias voltages exceeding a threshold of a few volts per centimeter the photosignal was seen to develop a long tail extending to several tens of microseconds. The

very long conduction-band lifetime deduced by Ohyama⁸ for electrons in InP under similar bias conditions is almost certainly a manifestation of the same effect. The threshold voltage for this tail was found to increase approximately linearly with applied magnetic field. The spectroscopic properties of the tail were investigated, together with the variation in tail shape and size with incident laser power.

An earlier rate-equation model for the process was critically examined, and its shortcomings pointed out. A model involving impact excitation and slow recombination between the ground impurity state, the conduction band, and other states (or groups of states) has been developed, and computer simulations based on this model are presented. The shapes of the initial pulses and the long-lived tail at $B=0$ and 3.75 T are seen to be faithfully reproduced by this model, together with the saturation behavior as a function of laser power. The fitting parameters required by the simulations are seen to be consistent with assignments of the N_2 population in the model to the $2p_-$ state and the N_3 population to the $2s$ state and with reported impact excitation cross sections and phonon decay rates.

ACKNOWLEDGMENTS

The experimental work was performed at the University of Nijmegen (Netherlands). We acknowledge the support of Stichting voor Fundamenteel Onderzoek der Materie (Netherlands), Science and Engineering Research Council (United Kingdom) for research support (A.A.R.) and for travel facilities (J.M.C.). We are indebted to D. Anderson and L. Taylor Royal Signals and Radar Establishment, Great Malvern, United Kingdom for generous gifts of samples, to G. Hill (United Kingdom Science and Engineering Research Council III-V Facility, Sheffield) for assistance with sample preparation, and A. van Etteger (Nijmegen) for designing the laser system. Several useful discussions with L. Eaves and J. C. Maan are also acknowledged.

*Present address: Department of Physics and Astronomy, State University of New York (SUNY) at Buffalo, Amherst, NY 14260.

†Also at Research Institute for Materials, University of Nijmegen, Toernooiveld, NL-6525 ED Nijmegen, The Netherlands.

¹J. M. Chamberlain, H. B. Ergun, K. A. Gehring, and R. A. Stradling, *Solid State Commun.* **9**, 1563 (1971).

²C. J. Armistead, P. Knowles, S. P. Najda, and R. A. Stradling, *J. Phys. C* **17**, 6415 (1984).

³A. A. Reeder, J. M. Chamberlain, R. J. Turner, and G. Hill, *Solid State Commun.* **57**, 355 (1986).

⁴K. K. Bajaj, J. R. Birch, L. Eaves, R. A. Hoult, R. F. Kirkman, P. E. Simmonds, and R. A. Stradling, *J. Phys. C* **8**, 530 (1970).

⁵C. R. Pidgeon, A. Vass, G. R. Allan, W. Prettl, and L. Eaves, *Phys. Rev. Lett.* **50**, 1309 (1983).

⁶G. R. Allan, A. Black, C. R. Pidgeon, E. Gornik, W. Seidenbusch, and P. Colter, *Phys. Rev. B* **31**, 3560 (1985).

⁷C. R. Pidgeon, G. R. Allan, A. Black, B. McGuckin, M. F. Kimmitt, and P. C. Colter, *Solid State Commun.* **53**, 1140 (1985).

⁸T. Ohyama, E. Otsuka, S. Yamada, T. Fukui, and N. Kobayashi, *Jpn. J. Appl. Phys.* **22**, L742 (1983).

⁹J. M. Chamberlain, A. A. Reeder, L. M. Claessen, G. L. J. A. Rikken, and P. Wyder, *Physica* **134B**, 426 (1985).

¹⁰L. Taylor and D. Anderson, *J. Cryst. Growth* **64**, 55 (1983).

¹¹H. J. A. Bluyssen and A. F. van Etteger, *IEEE J. Quant. Electron.* **QE-16**, 1347 (1980).

¹²J. C. Mann, Ph.D. thesis, University of Nijmegen, 1979 (unpublished).

¹³J. B. McManus, R. People, R. L. Aggarwal, and P. A. Wolff, *J. Appl. Phys.* **52**, 4748 (1981).

¹⁴Sh. M. Kogan, *Fiz. Tverd. Tela (Leningrad)* **4**, 2474 (1963)

- [Sov. Phys.—Solid State **4**, 1813 (1963)].
- ¹⁵G. L. J. A. Rikken, P. Wyder, and J. M. Chamberlain (unpublished).
- ¹⁶G. Ascarelli and S. Rodriguez, Phys. Rev. **124**, 1321 (1961).
- ¹⁷J. L. Robert, A. Raymond, R. Aulombard, C. Bousquet, and A. Joulie, in Lecture notes on Application of High Magnetic Fields in Semiconductor Physics, Wurzburg, 1976, edited by G. Landwehr (unpublished), p. 533.
- ¹⁸C. Trager, D. A. Cowan, and R. A. Stradling, Physica **134B**, 250 (1985).
- ¹⁹F. Brown, A. Anderson, and P. A. Wolff, Int. J. Infrared Millimeter Waves **1**, 277 (1980).
- ²⁰B. I. Shkiovskii and E. L. Efros, *Electronic Properties of Doped Semiconductors* (Springer, New York, 1984).
- ²¹*Landolt-Börnstein: Numerical Data and Functional Relationships in Science and Technology*, edited by D. Bimberg (Springer-Verlag, New York, 1982), Vol. 17, p. 281.
- ²²E. Scholl, J. Phys. (Paris) Colloq. **42**, C7-57 (1981).
- ²³N. F. Mott and H. S. W. Massey, *Theory of Atomic Collisions*, (Oxford University Press, Oxford, 1965).
- ²⁴W. Rosner, G. Wunner, H. Herold, and H. Roper, J. Phys. B **17**, 29 (1984).
- ²⁵G. E. Stillman, C. M. Wolfe, and J. O. Dimmock, in *Semiconductors and Semimetals*, edited by R. K. Willardson and A. K. Beer (Academic, New York, 1977), Vol. 12, p. 169.
- ²⁶K. Aoki, K. Miyamae, T. Kobayashi, and K. Yamamoto, Physica **117&118B**, 570 (1983).
- ²⁷J. Mannhart, R. P. Hubener, J. Parisi, and J. Peinke, Solid State Commun. **58**, 323 (1986).